IIETA International Information and Engineering Technology Association
Advancing the World of Information and Engineering

Journal Européen des Systèmes Automatisés
Vol. 59, No. 4, April, 2026, pp. 1029-1046
Journal homepage: http://iieta.org/journals/jesa

Improvement of Power Quality for Grid-Connected Microgrid Based Multsi-Source Power Systems Using an Integrated Load-Following – Artificial Neural Network Strategy

Sarmad Jasim Hasan[1*], Yaseen Saadi Abbas[2], Ahmed Zkear Abass[3]

[1] Wind Energy Department, Al-Nahrain Research Center for Renewable Energy, Al Nahrain University, Baghdad 10001, Iraq
[2] Electronic and Communications Engineering Department, College of Engineering, Al Nahrain University, Baghdad 1001, Iraq
[3] Department of Electrical Engineering Technology, Ibn Khaldun Private University College, Baghdad 1001, Iraq

Corresponding Author Email: sarmad_jh@nahrainuniv.edu.iq

https://doi.org/10.18280/jesa.590414

Received: 12 November 2025
Revised: 9 March 2026
Accepted: 14 April 2026
Available online: 30 April 2026

Keywords:
energy management strategy, renewable energy, photovoltaic system, load-following, artificial neural network, electric vehicle, ECE-Urban drive cycle

ABSTRACT

This article proposes a novel energy management strategy (EMS) designed to optimize power quality in renewable multi-source microgrids (MG), including electric vehicle (EV) energy consumption. The proposed MG integrates a solar photovoltaic (PV) system, EV load profiles, an energy storage unit (ESU), and a grid-connected source, aiming to enhance power quality under varying power generation and load consumption conditions. The integration of load-following (LF) with an artificial neural network (ANN)-based EMS is presented to optimize power sharing and regulate the direct-current (DC) bus voltage under transient load conditions. Unlike conventional voltage-control methods, the LF-ANN approach introduces a smart EMS that dynamically generates battery power references and coordinates power sharing among the PV source, battery energy storage system (BESS), EV load, and the utility grid under state-of-charge (SOC) constraints, while maintaining stable DC-link voltage during rapid changes. The EV load profile is modeled using the ECE-Urban drive cycle to represent consumption. The DC/DC boost and bidirectional converters connect the PV system and the ESU storage to the DC bus link, respectively. The proposed EMS framework is simulated in the MATLAB environment and tested under various irradiance, load demand, and battery charging scenarios. Results show that the LF-ANN method ensures DC bus voltage stability, reliable optimal power flow, and extended battery life. Comparative analysis with the classical LF-PI (proportional-integral) method demonstrates superior performance in terms of settling time, overshoot, and rise time of DC bus regulation, establishing the proposed EMS as a promising solution for renewable MG operations with EV integration.

1. INTRODUCTION

The growing adoption of electric vehicles (EVs), along with renewable energy technologies, is a global effort towards a cleaner and more sustainable energy system [1]. Consequently, direct-current (DC) microgrids, which include distributed energy resources (DERs) like photovoltaic (PV) panels, wind turbines, and energy storage systems (ESS), are emerging as advanced frameworks for controlling local power generation, storage, and consumption [2, 3]. The major important problems in such systems it the provision of a robust and intelligent EMS to control the power sharing between the sources and the EV battery and enhance the system reliability and minimize the cost of operation [4]. However, the EV charging stations may increase the demand of load integrated with the grid and cause unpredictable consumption issues. The used EMS methods in the latest few years are presented to solve this issue in the modern microgrids. Artificial Intelligence (AI) is capable for modeling complex systems, forecasting states, and optimizing multi-objective functions under uncertain conditions [5]. However, the incorporation of Vehicle-to-Grid (V2G) and Grid-to-Vehicle (G2V) systems along with PV systems has become crucial for improving the flexibility, reliability, and sustainability of modern power systems. The global adoption of solar energy and EVs enables them to be coupled through a bidirectional exchange of energy. This integration smartly addresses challenges linked to energy intermittency, grid stabilization, and energy optimization [6, 7]. G2V or Grid to Vehicle refers to conventional charging of EVs from the power grid. When integrated with PV systems, G2V enables EVs to charge during peak solar generation periods. Reducing the use of fossil fuels is directly linked to the reduction of greenhouse gas emissions. EVs may take advantage of advanced charging protocols by automating the charging process during peak PV output periods, thus avoiding energy waste. It helps mitigate the intermittency of solar energy while aiding in peak load shaving, voltage regulation, and frequency support. The collaboration of PV, V2G, and G2V technologies helps solve one of the major challenges in renewable energy systems intermittency. Changing weather and daily solar cycles contribute to making solar energy unpredictable. V2G-enabled

EVs provide portable storage that can capture surplus solar energy and discharge it during periods when generation is minimal. This lessens the dependency on centralized ESS and increases the self-consumption of solar energy in homes or community microgrids, integrated G2V and V2G functions managed together can contribute to demand response and load balancing tasks [8-10].

In literature, several EMS methods are proposed for microgrid with integrated EV charging stations guided by advanced AI technologies; EMS based optimization including ANN, fuzzy logic, adaptive neuro-fuzzy system (ANFIS) and other metaheuristic optimization algorithms. The objectives of these EMS are to manage a coordinated flow of energy between RES, ESS, and EV loads, performing strategic optimization considering price signals, grid interaction rules, battery state of charge (SOC), and user-tailored settings. The authors in the study [11] proposed adaptive EMS based ANFIS algorithm to control the V2G power flow including the RES and variable EV charging/discharging process. To achieve the goal of using more energy within the building while simultaneously lowering energy related expenses, they concentrated on developing a control system with a real-time adaptive hierarchy that responds to changes in the grid's structure. Due to the self-tuning capability of ANFIS, its convergence and accuracy in predicting load and generation schedules surpasses that of standard fuzzy systems. This technology advantage stems from ANFIS's hybrid learning strengths. The applied EMS concepts improved load balancing efficiency by 26.8%, slashing operational costs by almost 18% in comparison to conventional approaches. These ideas were also expanded on by Sathyan et al. [12], who designed a dedicated ANN-based EMS for EV charging stations powered by PV with batteries and V2G features, concentrating on real-time energy distribution and cost optimization during fluctuating solar irradiance and EV dynamics. Their architecture incorporates renewable generation forecasting, EV charging demand prediction, and the multi-layer feedforward ANN trained on historical data for energy storage optimization. The strength of this system is enabling preemptive action on energy balancing and optimizing resource distribution to reduce load and enhance voltage-standby control. Simulation results revealed that their proposed EMS achieved a solar energy utilization enhancement of 23.6% and a peak grid power demand reduction of 21.4%.

Shamami et al. [13] designed an artificial intelligence-driven EMS dedicated to V2G applications focusing on improving energy consumption and costs, alongside sustainability in residential power systems. The system displayed significant performance enhancement: simulations showed 22% improvement in renewable energy self-use. Furthermore, there was a 17% drop in energy costs compared to an EMS reliant on conventional rules. Following this, Singh et al. [14] proposed an AI-based adaptive controller for coordinated V2G and G2V operation at EV charging stations. The goal was to design an automated deep learning model capable of self-adjusting energy flow in both directions for battery longevity, optimal energy pricing, and grid support services. Their approach uses feedback loops in real-time along with adaptive decision mechanisms to reinforce charge and discharge processes important for grid-dependent and intermittently solar-dependent systems. An important benefit of this development stems from the fact that the controller reacts not only to changes in demand and tariff rates but also to the vehicle's SOC and user-set boundaries, making it internally adaptive. Collectively, these contributions emphasize the game-changing impact artificial intelligence technologies can bring to energy management systems with regard to efficiency improvements in vehicle-to-home and vehicle-to-grid configurations. These methods enhance overall system productivity while simultaneously increasing the economic and environmental benefits of integrating EVs into decentralized energy systems by adding adaptive learning and intelligence forecasting into system control. This is important for designing future architectures of energy management systems aimed at evolving towards the next level of smart energy ecosystems that are resilient and low-carbon. The authors in the study [15] presented a smart EMS algorithm capable of optimizing the interaction between solar PV arrays, EV chargers, and the main grid to reduce operating costs and improve the utilization of renewable energy sources. The applied strategy was tested and validated under real-time solar irradiance, forecasted EV charger arrival time, and costs of the energy consumption. The used approach provides prospects for enhanced systems with demand response and grid integration to offer ancillary services beyond billing requirements. Based on simulations, the performance analysis showed that energy cost containment with smart control increased to 18.5% while grid peak load decreased by 21.7%, illustrating the significant impact of smart controls on energy management systems. These works illustrate the importance of smart EMS algorithms and storage technologies to enhance the operation of PV powered EV charging stations. Furthermore, they show how advanced control strategies and energy storage increase the resilience and sustainability of EV charging infrastructure essential for future renewable energy-based decentralized power grids and electrified public transport in cities. As the adoption of EVs and PV systems increases, the energy EMS for charging stations have garnered interest regarding their efficiency and support to the grid. A smart EMS for a gird-connected solar powered EV charging station was designed by Haque et al. [16] to tackle this important problem. Their solution seeks to streamline energy management among solar production, EV loads, and grid interactions in order to enable charging, reduce energy costs and lower grid peak demand. Solar irradiance, EV arrival patterns, and time-of-use pricing offered as inputs, the EMS algorithm executed charging as well as grid exchange optimally. The system is designed to respond to economic signals, which enable demand response capable operations. Simulations showing a reduction of peak grid load and of overall energy cost from unmanaged charging configurations demonstrated the effectiveness of this approach.

In the study done by Amir et al. [17], an intelligent EMS was used to build the coordinated multi-level control framework in PV integrated charging stations targeting peak load reduction and enhancement of power quality further. Their model proposes the design of a multilayer control system with real-time data processing, load prediction, and control forecasting alongside optimal power scheduling. In contrast to static models of EMS, this intelligent model considers EV traffic as well as generation and load change, which greatly enhances control flexibility over multi-source energy coordination. To manipulate the complex energy interactions between several EVs and changing PV output, the system responds quickly and is highly scalable as a multi-source EMS framework is used. Moreover, the need to improve the integration of renewables and storage is a driving factor in the

development of new generation intelligent energy systems. Kouka et al. [18] implemented a dynamic management system to control the charging cycles of EVs at PV powered charging stations. Their simulations with different solar irradiation profiles increased the PV energy use, with a decrease in energy imported from the grid, which proved the system's efficiency when operating in off-grid and semi-grid modes. In a different context, Yaqoob et al. [19] were concerned with the problem of hybrid ESS and provided an efficient flatness-based energy management for systems that incorporate supercapacitors (SC) with lithium-ion batteries. Their study focused on EV fast charging as well as other high-power applications where energy distribution improvements and lifespan optimization combined with swift dynamic response were critical. Transitory load change responsiveness is particularly high in their work because power flow management between hybrid storage elements utilizes differential flatness theory, one of the major innovations. A significant benefit of this approach is the ability to accurately predict energy distribution with minimized computations due to its model-based predictive control feature. The authors in the study [20] developed a real-time EMS strategy for hybrid system configuration. This is analogous to the practical challenges faced in grid-connected EV charging infrastructure systems. Their research focused on the realization of a control architecture that aims to provide an uninterrupted power supply during transient outages by managing ESS while enforcing critical load prioritization for essential loads. Although shipboard systems may differ from EV charging systems in topology, the speed and agility with which the hybrid EMS responds to high demand and fluctuating inputs is exceptional.

Rezk and Ghoniem [21] proposed a control method aimed at optimizing load sharing between lithium-ion batteries and SC in vehicle systems. The goal was to prototype systems that alleviated the challenges faced by battery systems during rapid acceleration and deceleration by leveraging the supercapacitor's high power output and fast reaction capabilities. Their findings suggest that SC are capable of absorbing high-frequency load components while batteries supply the lower frequency steady-state load. As a result, thermal stress and SOC oscillations were diminished in the battery, leading to improved system longevity and energy efficiency. The authors in the study [22] proposed an intelligent battery management system (BMS) designed for PV-powered solar EVs. This intelligence-based fuzzy logic provided the ability for the system to reconfigure its charge-discharge cycles based on real-time PV generation, user demand, and battery health indicators. Furthermore, the intelligent BMS facilitated more controlled energy transfer between the solar array and EV drivetrain, improving the system's capacity for autonomous and efficient operation during intermittent solar radiation. These results highlight the capabilities of AI-infused BMS not only to enhance functionality but also to act as cornerstones for more sophisticated energy management frameworks in PV-EV systems. Addressing the critical issues of battery safety and lifecycle management, coordination of renewables, and system intelligence.

This paper presents a new EMS by integrating the ANN-with load following technique for a hybrid power system by taken into account the charging BESS and EV load consumption. The used method aims to stabilize the DC bus voltage and optimization the power source of the system with their constraints. The grid tied system was managed to export and absorb the active power during the simulation cases, which provide more minimizing the operation cost.

The main contributions of the study are:

1. Proposing a new LF-ANN EMS for an EV-integrated renewable microgrid, which allows intelligent coordination of power flow among PV, BESS, the grid, AC load, and EV demand.
2. Design a comprehensive hybrid DC/AC grid-connected microgrid model comprising PV generation, DC-link dynamics, bidirectional battery converter, inverter interface, and EV load profile is realized in MATLAB/Simulink.
3. By leveraging only two input variables (DC-bus voltage error and battery SOC), a power reference for the battery is derived by a computationally efficient ANN controller. Thus, the proposed EMS can be implemented in real time with less tuning effort compared to complex optimization-based EMS methods.
4. The LF-ANN EMS proposed here is demonstrated through the operating conditions with variable irradiance and EV/load variations. The performance is evaluated by the quantitative such the DC-link overshoot/undershoot, PV self-consumption, grid power factor (PF), and current THD, thus presenting reproducible evidence of effectiveness.

2. PROPOSED SYSTEM MODELING

The proposed DC/AC microgrid is shown in Figure 1. The entire system complements are a solar PV system, ESU DC/AC converter, EV load profile, three phase AC load, and utility grid. The PV system is connected to the DC bus via DC/DC boost converter, which adjusts the MPP via MPPT tracking method. The ESU is controlled using a bidirectional DC/DC converter that adjusts the charging or discharging of the battery energy storage system (BESS). The EV load profile used in this work is based on the ECE-15 Urban drive cycle, which represents the vehicle speed. In addition, the system is connected to the grid via 0.4 KV/33 KV transformer via 33 KV, 50 Hz utility grid.

2.1 Solar photovoltaic system modeling

Figure 2 shows the single diode model of a PV module or array. This model describes the electrical behavior of the solar system. The equation that describes the current-voltage (I-V) characteristics of a solar cell/module using the single-diode model is as follows [23]:

$$I_{pv} = N_P I_{ph} - N_P I_o \left[exp\left(\frac{V_{pv} + R_s \left(\frac{N_S}{N_P} \right) . I_{pv}}{\alpha V_{Th} N_S} \right) - 1 \right] - \frac{V_{pv} + R_s \left(\frac{N_S}{N_S} \right) . I_{pv}}{R_{sh} \left(\frac{N_S}{N_P} \right)} \quad (1)$$

where,

- I_{pv} is the output current (photocurrent).
- V_{pv} is the output voltage.
- I_{ph} is the photocurrent generated by the cell.
- I_o is the reverse saturation current of the diode.
- α is the diode ideality factor.
- R_s is the series resistance.
- R_{sh} is the shunt resistance.
- V_{Th} is the thermal voltage, approximately 25.85 mV at room temperature (T = 25 °C).
- N_S is the number of series modules.
- N_P is the number of parallel strings of array.

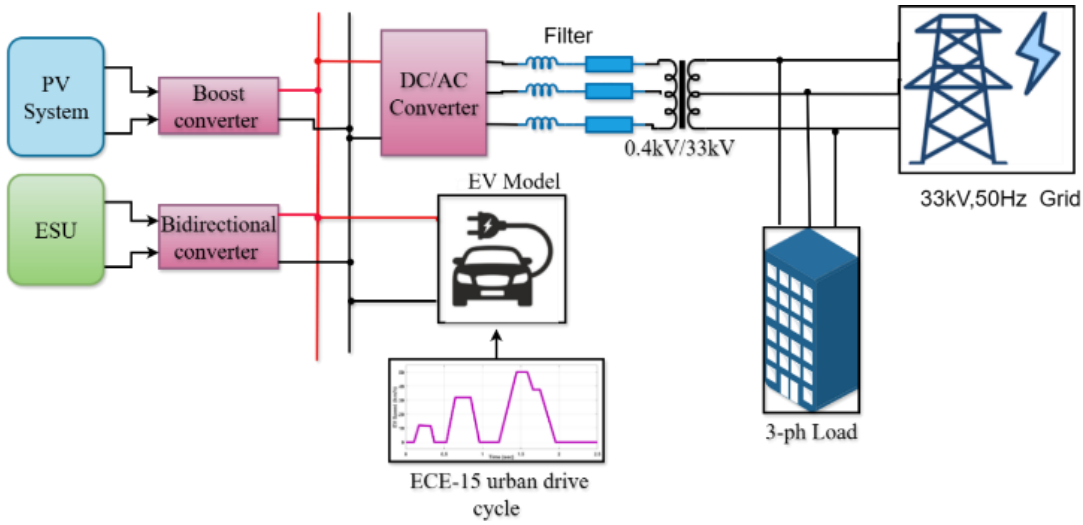

Figure 1. Proposed system-based microgrids (MG)

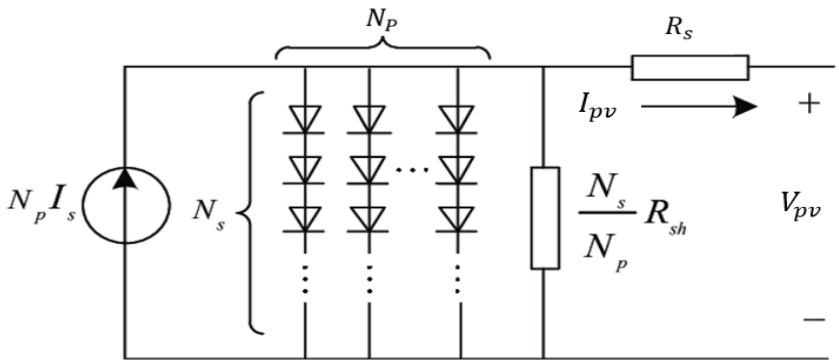

Figure 2. Solar array model

2.2 EV modeling

The mathematical equation of the total motor force of the vehicle can be expressed as follows:

$$F_T = F_m + F_r + F_{ad} + F_U \tag{2}$$

where, F_m represents the motor force, F_r is the rolling resistance force, F_{ad} represents the aerodynamic force, and F_U represents the grade ability force. These forces can be expressed as follows [17]:

$$F_m = \left(M_v + J_{em} \frac{\rho^2}{R^2} \right) \frac{dv(t)}{dt} \tag{3}$$

$$F_r = C_r M_v g \cos(\alpha) \tag{4}$$

$$F_{ad} = 0.5\, \rho\, v^2 A\, C_d \tag{5}$$

The parameters of the above equations can be defined as:

- M_v is the vehicle mass.
- J_{em} is the inertia of the motor.
- ρ is the air density.
- R is the tire radius.
- C_r is the rolling friction coefficient.
- g represents the gravity acceleration.
- α is the road slop.
- v is the vehicle speed.
- A is the frontal area.
- C_d is the aerodynamic drag coefficient.

However, the load power produced by the traction engine on the DC link ($P_L(t)$) is written as follows [17]:

$$P_L(t) = F_T(t) \times v(t) \times \eta_t \tag{6}$$

where, η_t is the mechanical transmission efficiency.

The abbreviated form of the urban driving cycle, i.e., the ECE-15, is used to represent the EV load. The ECE-15 model was shown in Figure 3. Moreover, the driving cycle has been carefully crafted to capture the inherently dynamic nature of

urban driving conditions, involving numerous phases of acceleration as well as deceleration, and segments of idling. All of such driving activities translate into time-varying power requirements that must be properly managed by the system for peak performance. By using the ECE-15 driving profile along with system operating conditions, the authors of this paper model their EMS response to real variations in the power demand of an electrically powered vehicle (EV). Moreover, the used EMS can perform under heavy load changes, keep the DC-bus voltage stable, and manage the power flow between the PV source, BESS, and the grid.

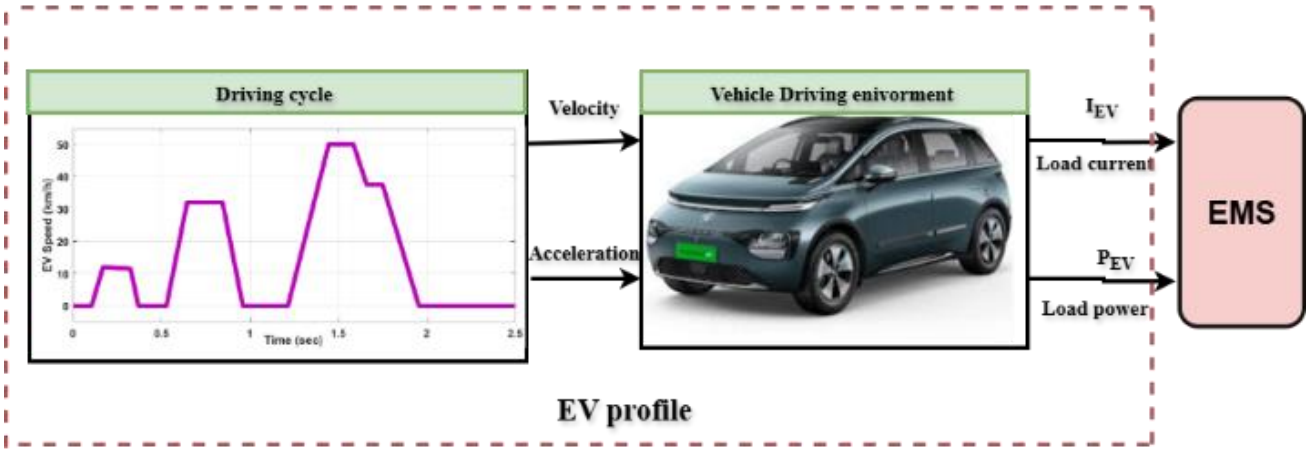

Figure 3. Electric vehicle (EV) profile-based reduced ECE- driving cycle

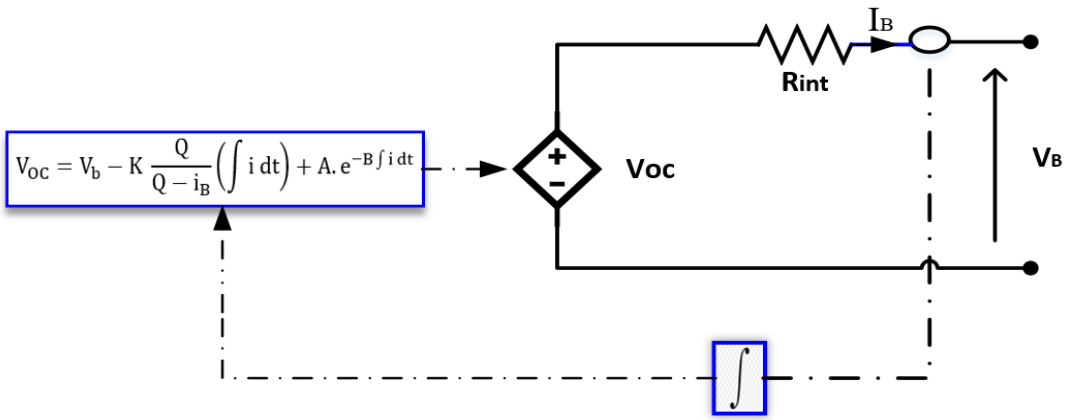

Figure 4. Electrical model of the lithium battery

2.3 Energy storage unit

The ESU under consideration here depends upon battery energy storage systems (BESS) to effectively reduce power swings and supply/output for the microgrid's stableness [24-26]. Batteries possess the answer to combat the intermittency of renewable sources of energy, i.e., the PV sources, by conserving excess generated energy at high-solar-irradiation moments and releasing energy at maximum demand or low-generation moments. This helps significantly to enhance system flexibility and reliability. In this regard, lithium-ion (Li-ion) batteries are chosen due to the high-energy storage capacity or high energy density, higher cycle life, higher efficacy, and fast response to transients of load conditions. Advanced BMS actively monitors and controls SOC, and voltage, and temperature of the battery and thereby ensures safe functioning and maximization of the lifetime of the battery [26].

The battery system functions at pre-defined SOC levels (say, 20% to 90%) and inhibits deep discharges and overcharges and thereby sustains the lifespan of the battery and achieves optimized functioning. The interfacing of the battery ESS with the energy management system surely enhances renewable energy penetration and minimizes dependence upon fossil-fuel-based backup sources and minimizes operating expenses and adverse environmental effect and achieves sound microgrid stableness. The SOC battery equation is expressed as [24]:

$$SOC_{bt}(t) = SOC_{bt}(t_o) + \frac{1}{C_n}\int_{t_o}^{t} i_{bt}(t) \tag{7}$$

where, $SOC_{bt}(t_o)$ is the initial SOC of the battery, C_n is the nominal capacity of the EV battery. Figure 4 shows the electrical model of the lithium battery.

Figure 5 illustrates the suggested ESU control scheme. The ESU integrates consists of the bi-directional DC-DC converter, which functions under the diligent supervision of a suggested EMS along with a Pulse Width Modulation (PWM) generator. However, the BESS basically depends on functioning as a dynamic energy buffer; it can uniquely absorb the surplus energy that can be unconventionally produced, e.g., from solar panels, or, on the other hand, release power to the whole system when there is a lack of energy. The bi-directional converter plays an enormous and vital role in that

it enables two-way power flow, which can be transferred by its two operating modes. In the boost mode operation, the converter enables the battery to be charged by increasing its voltage level when there is a large amount of excess energy available; such operation guarantees that the excess energy is exploited efficiently.

The coordinated control plays a significant role towards ensuring that there remains effective power exchange, as well as stability of the DC bus voltage. Additionally, it benefits the battery through minimizing instances of overcharging or deep discharging of the battery pack. Thus, the EMS ensures improved system reliability as well as responsiveness of the energy system.

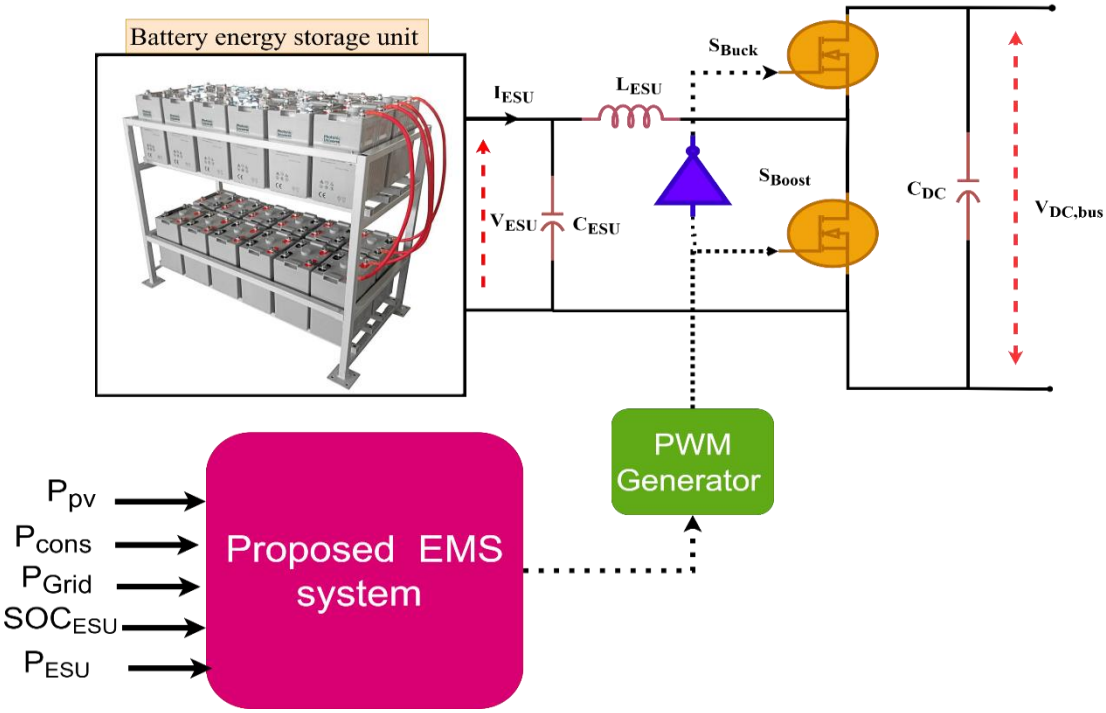

Figure 5. Energy storage unit (ESU)-based microgrid system

3. PROPOSED ENERGY MANAGEMENT STRATEGY

The proposed EMS aims at controlling power flow within a grid-connected renewable energy system consisting of PV generation, bidirectional-based BSU, and a variable DC-link bus. MATLAB/Simulink is used for modelling the EMS to stabilize DC bus voltage stability and control the power balance between the storage, grid, and EV load. The objectives of the suggested EMS include prioritizing self-use of PV source, the EMS accompanied by battery SOC limitations and grid support. This EMS strategy integrates an LF with the ANN method. The DC bus is controlled at 700 V with DC bus voltage controller. The net battery power reference is provided by the EMS such as the incompatibility of the load demand with the combined available power supplied by grids and PV. The modeling of the system is conducted based on the following equations [27, 28]:

$$P_{Cons} = P_{AC\_Load} + P_{EV} \tag{8}$$

$$P_{ESU,ref} = P_{Cons} - (P_{pv} + P_{Grid}) + \frac{d}{dt}V_{bus} \tag{9}$$

$$I_{ESU,ref} = \frac{P_{ESU,ref}}{V_{ESU,ref}} \tag{10}$$

where, P_{Cons} is the total consumption power of the system, $P_{ESU,ref}$ is the reference power of the ESU, P_{Grid} is the active power of the utility grid, P_{AC_Load} is the three-phase load power. Also, the P_{EV} is the consumption power via EV, $V_{ESU,ref}$, and $I_{ESU,ref}$ are the voltage and current drawn by the EV. The reference power Pb_ref, is converted into a current reference, which is termed as I_{bref}. The current reference is subsequently compared with the real battery current, which is termed as Ibt, in order to determine any deviations. The duty is used to successfully control the charging and discharging current of the battery. The ANN controller estimates Vbus' in order to control the voltage of the DC-link and estimate the SOC of the battery. However, the classical proportional-integral (PI) control is written in Eq. (11) [29].

$$\frac{d}{dt}V_{dc,bus} = k_p \times e + \frac{k_i}{s} \times e \tag{11}$$

The error of the bus voltage is represents by $e = (V_{dc,ref} - V_{dc,bus})$, where $V_{dc,ref}$ is the reference value of the DC bus voltage $V_{dc,ref} = 700\,V$, k_p and k_i are the proportional gain and integral gain of the PI controller.

The proposed ANN and the classical PI controllers for LF-EMS are shown in Figure 6, where the derivate of the bus voltage entered the LF blocks to produce the desired battery power. To implement ANN controller in this research, it is adopted as a feedforward neural network placed alongside the EMS based on LF. The ANN inputs are (i) DC bus voltage error $(V_{dc,ref} - V_{dc,bus})$ and (ii) battery SOC for the ANN to provide voltage regulation while complying with battery usage limitations. The output of the ANN is the control signal, which

is used to regulate the DC-link within the EMS framework. The ANN is composed of a single hidden layer with 10 neurons, and the training was performed offline by using the Levenberg-Marquardt backpropagation algorithm (trainlm). The training goal is to reduce the mean squared error (MSE) as much as possible between the ANN output and the control action desired, which is obtained from the EMS reference behavior under various simulated scenarios of operation (variations in irradiance and load). Moreover, the block diagram of the suggested EMS is shown in Figure 7. The sub-system of the SOC control scheme was shown in Figure 8.

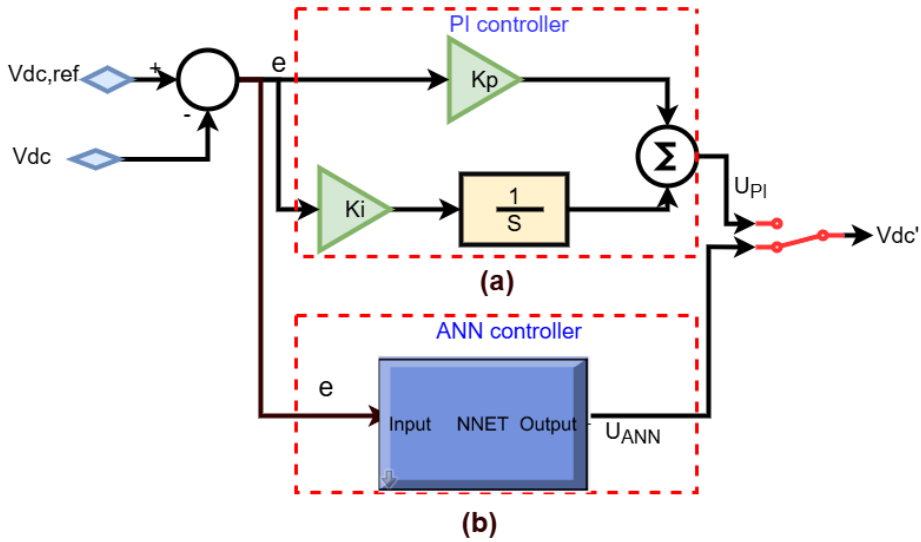

Figure 6. (a) Classical proportional-integral (PI) controller [29], (b) proposed artificial neural network (ANN) controller for load-following-energy management strategy (LF-EMS)

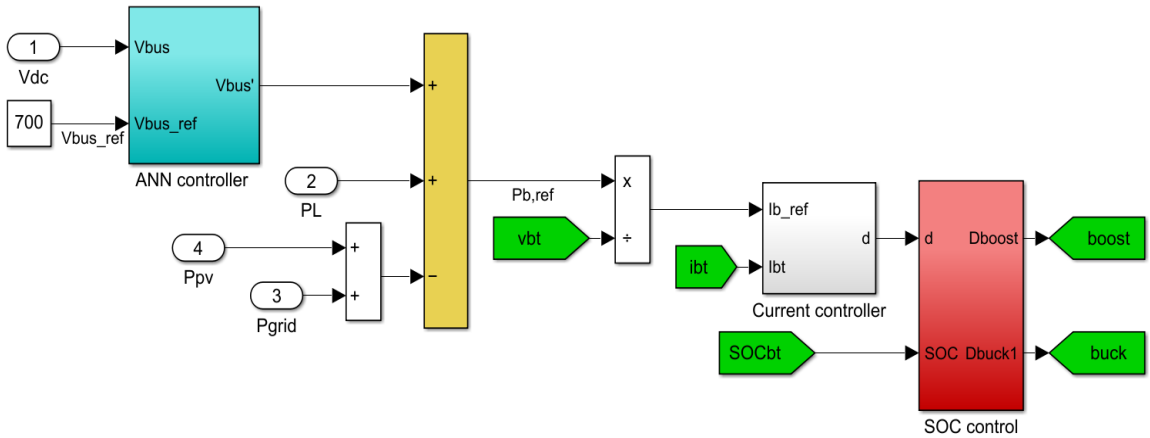

Figure 7. Load-following-artificial neural network (LF-ANN)-energy management strategy (EMS) MATLAB simulation

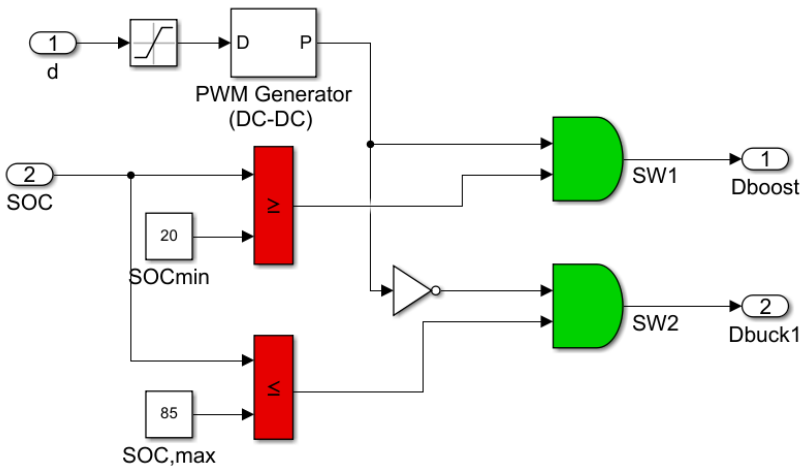

Figure 8. Sub-system of the state-of-charge (SOC) control scheme

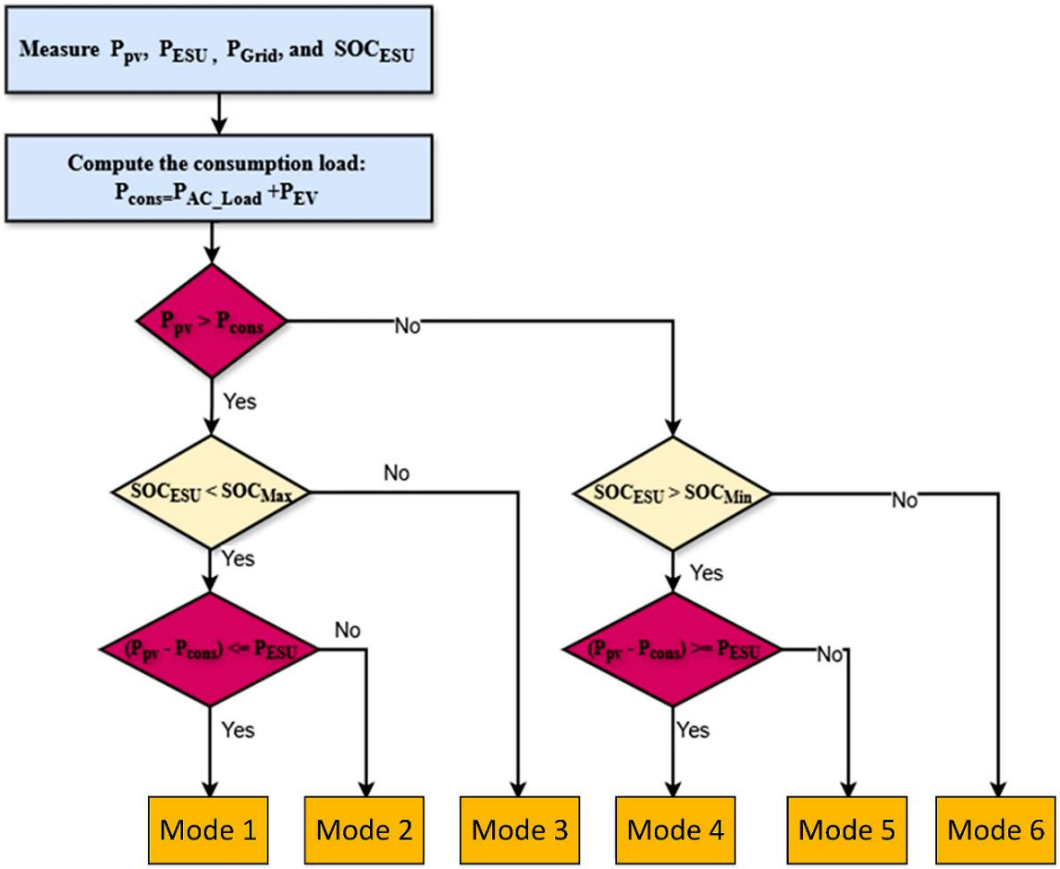

Figure 9. Flowchart of the proposed energy management strategy (EMS)

The flowchart of the suggested EMS is shown in Figure 9. The modes of the operation of the proposed EMS are presented as follows:

Mode 1: PV surplus → Battery charging (Grid idle);

PV generation is first used for the load and the excess component is utilized for charging the BESS (within the SOC limits). Thus, the power exchange with the grid is kept at a minimum.

Mode 2: PV surplus exceeds battery limit → Battery charging + Grid export;

PV generation is first used to meet the load then BESS is charged at the allowable limit and the remaining surplus after charging the battery is exported to the grid.

Mode 3: PV deficit → Battery discharging (Grid idle);

When there is not enough PV generation, the BESS is used to meet the shortfall by discharging while still keeping within the SOC constraints.

Mode 4: PV deficit + BESS reaches discharge limit → Grid import;

In case there is little PV generation and the BESS is not allowed to discharge further due to SOC limits, the rest of the deficiency is covered by grid import.

Mode 5: SOC upper bound reached → Battery charging is stopped, Grid export if surplus exists;

Once the SOC hits the maximum threshold, battery charging will be shut off and any unused PV power will be fed back to the grid.

Mode 6: SOC lower bound reached → Battery discharging is stopped, Grid import to supply demand.

Upon the SOC reaching the minimum limit, the discharging of the battery will be stopped and the grid will provide the rest of the load demand.

4. RESULTS AND DISCUSSION

The simulation results of the proposed work are obtained using MATLAB/Simulink software. The proposed EMS was verified and tested under different case studies to prove the performance of the proposed EMS. The parameters of the system are listed in Table 1. The case studies are discussed as follows.

4.1 Case study 1: Variable irradiance evaluation with consumption EV load

Figure 10 shows the profiles of solar irradiation, temperature, EV drawn EV current, and SOC of the BESS. As shown in this figure, the simulation time interval was taken for 2.5 seconds. The irradiance was changed during this duration to show the increasing or decreasing the PV generation. The noticeable decrease in irradiance levels is significant, since it drops considerably from its initial measurement of 900 W/m² to 500 W/m², showing a considerable decrease in solar resource availability. Despite these unexpected and abrupt changes, the designed EMS, is capable of taking over and immediately responding to these changes. Hence stabilizing the operation. In this case, study, the PV temperature keeps constant with 25 °C degree. The current drawn by the EV load is varied as presented in Figure 10(c). This figure gives a detailed and complete description on the charging current profile of the EV during consumption duration. Moreover, the proposed EMS is responsible for controlling and managing power interchange from the battery to the EV. Thus, a high-magnitude levels up to 200 A can be achieved without instability for the trajectory of the SOC. Therefore, the SOC goes through a highly precise evolution throughout the entire

duration of the test situation. Even with the dramatic reductions in irradiance and the intermittent nature of charging for EVs, the SOC is found to hover in an extremely tight and stable band ranging from 69.9995% to 70.002%.

Table 1. Simulation parameters of the system

Components	Parameter	Value
Photovoltaic (PV) system	P_{pv}	365 W
	V_{pv}	39.5 V
	I_{pv}	9.25 A
	N_p	52
	N_s	8
Battery energy storage system (BESS)	C_n	60 Ah
	SOC_{bt}	70 %
	V_B	400 V
Electric vehicles (EVs)	M_v	700 kg
	C_d	0.29
	ρ	1.225 kg/m^3
	R	0.2 m
	C_r	0.009
	g	9.81 m/s^2
	A	2
Utility grid	Grid voltage	33 kV
	Grid frequency	50 Hz
	Filter inductance	2.5 mH
	Filter capacitance	2 uF
DC/DC boost converter	Inductance	1 mH
	DC bus capacitance	12 mF
	Switching frequency	5 kHz
Bidirectional converter	Inductance	1 mH
	capacitance	100 uF
	Switching frequency	5 kHz

The obtained results in terms of DC bus voltage, active power of all sources, injected AC current of grid, and dq-axis currents are illustrated in Figure 11. In this figure, the DC link voltage demonstrates the ability of the presented LF-ANN based EMS strategy to tightly control the measured voltage to its desired value (700 V). Therefore, the presented deviation in the voltage less than 2% even with the high transient consumption EV load, and PV generation fluctuations. This confirms the fast response and optimal power sharing via the applied EMS response. As observed in Figure 11(b), the active power of the grid is changed from positive sign to negative when the consumption power more the generation during the reduction the solar irradiation. The BSU reference power discharges the DC bus based on ots SOC value while the excess power is transferred to grid when the irradiance is high. The difference between the PV power and the consumption is used to charge the BSU or exported to the utility grid via DC/AC converter. As a result, the obtained results show that the recommended EMS ensures a high optimization ability to regulate the bus voltage and controls the RES production. Figure 11(c) displays the AC injected current to the grid during this scenario. The peak RMS current value is 2.3 A.

The EMS controls the export and import operations of the grid based on the PV generation. The smooth changes in current show that the grid-side converters and local resources are working together well without causing harmonic distortion. Figure 11(d) shows the dq-axis currents, when power is exported or absorbed from the grid. As shown in the I_d, it is identical to the reference value of $I_d = 1\ A$ and its value changes from positive to negative when power is injected into the grid, and the current turns to the negative part when power is absorbed from the main grid. Furthermore, the q-axis of the reactive power $I_q = 0\ A$.

Figure 12 shows the active and reactive power of grid, high voltage side of grid and 3-ph load current. The active power value varies depends the PV generation and load power as shown in time interval 0 seconds to 1 seconds, where the active power is positive (100 KW) which means the required power for the BSU and consumption in the 3-ph load and EV model is covered by the PV system. After that, when the consumption load of EV increases at time 1.4 sec, the active power is absorbed from the grid. During this transient, the reactive power of the system is zero, which confirms the reliability of the proposed EMS. The grid voltage at right side of the transformer still constant with 33 KV. The power drawn from the load also constant with peak ac value about 85 A.

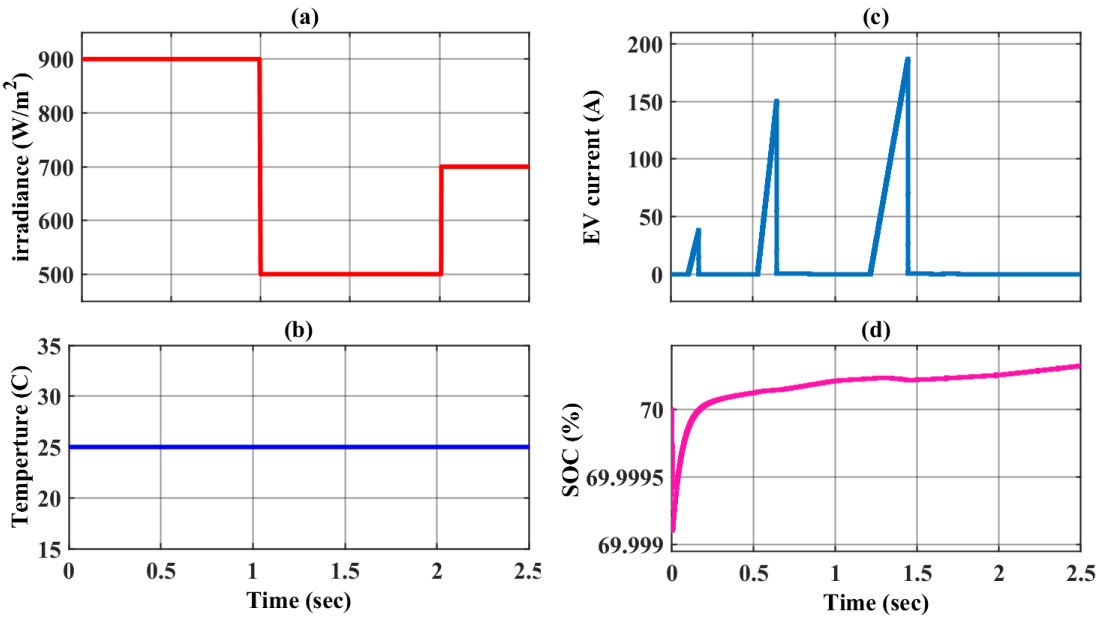

Figure 10. (a) Irradiance graph, (b) temperature, (c) electric vehicle (EV) current, (d) state-of-charge (SOC) of the battery

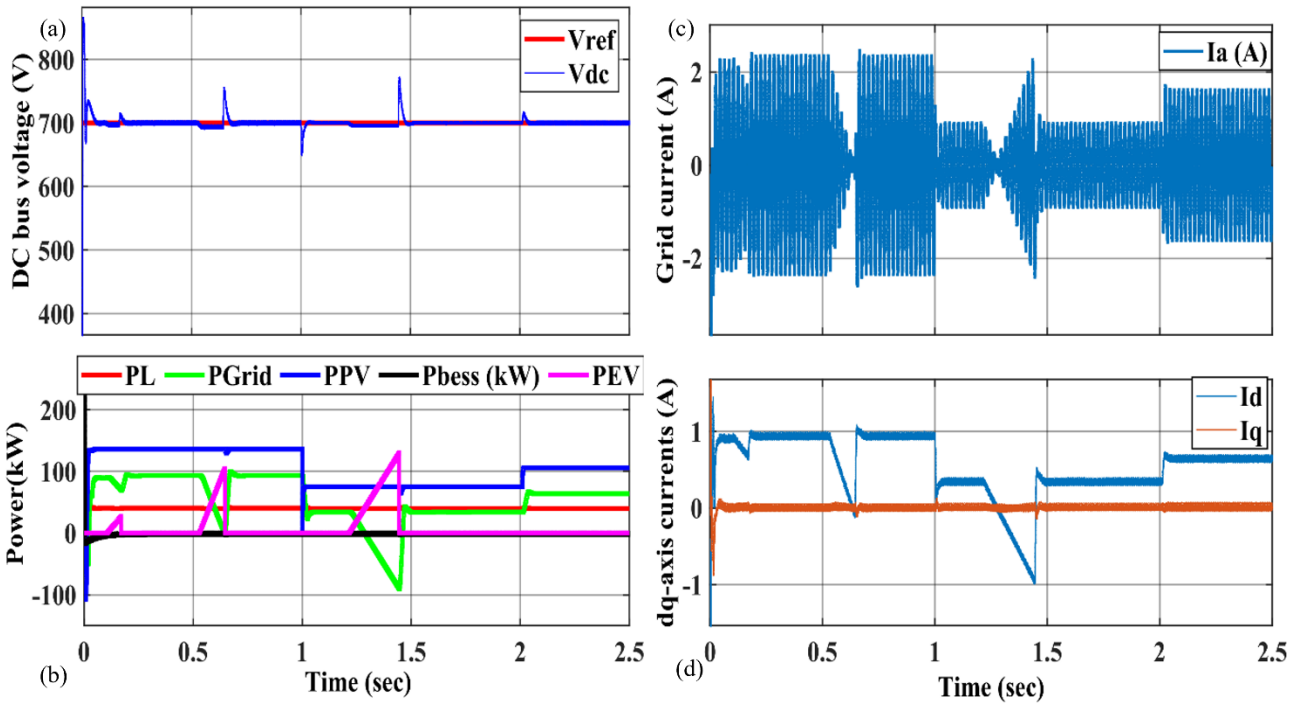

Figure 11. (a) Direct-current (DC) bus voltage (b) active power of system (c) injected current to grid (d) dq-axis currents

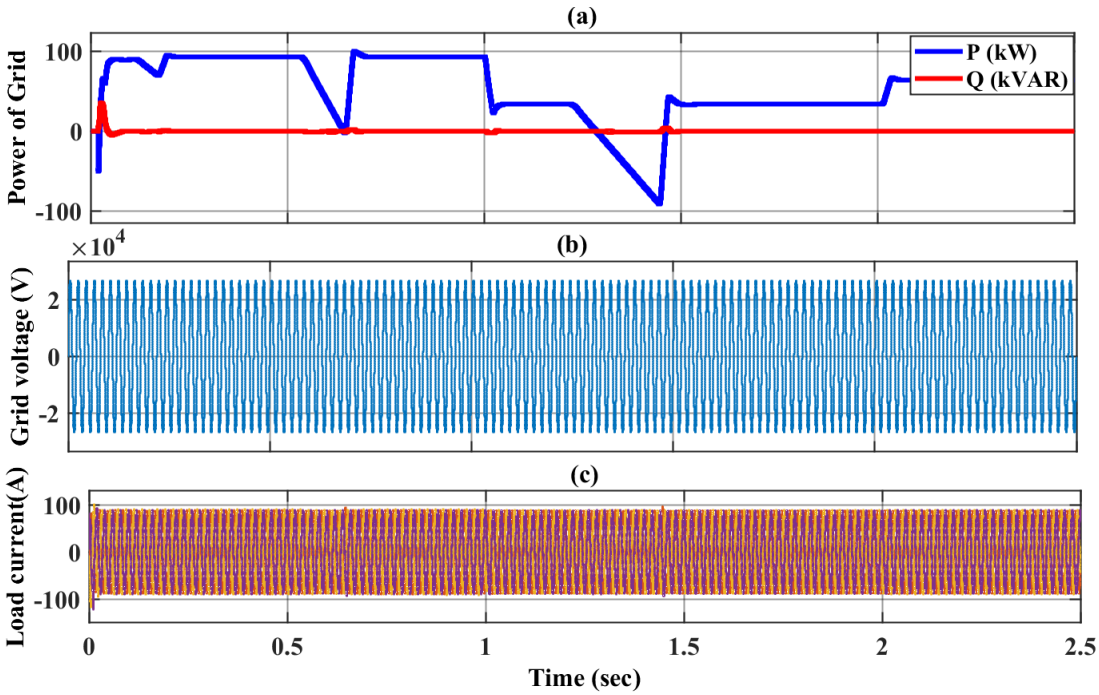

Figure 12. (a) Active and reactive power of grid, (b) high voltage side of grid, (c) 3-ph load current

Figures 13 and 14 display the grid current with voltage under scenario 1. The grid voltage is scaled by $V_a/5000$ for plotting with the corresponding AC current (I_a). The zoomed values as seen in Figure 14 during small interval time of ($1.93\,sec - 2.1\,sec$) are presented to show the current reduction or increasing. The grid current value about $\pm 1.6A$ with pure sinusoidal waveforms. The phase shift between the voltage and current is zero and this means the power factor of the inverter is unity. This result confirms the bidirectional power flow from the inverter to grid. Also, the sinusoidal shape of current and the absence of harmonic distortion demonstrate compliance with IEEE 519 current quality standards. Table 2 reports the obtained results at case study 1. The achieved results demonstrate that the latest LF ANN EMS can still tightly regulate the DC-link voltage very efficiently despite moderate operating variations. The DC bus voltage is always maintained very close to the setpoint (700 V) with limited overshoot and undershoot; hence, control improvement is confirmed through enhanced damping and faster recovery as compared with the conventional one. Additionally, the grid reactive power is kept nearly at zero level; therefore, the power factor is almost unity (PF > 0.99), which is proof of the power quality improvement objective. The grid energy exchange reveals that the import energy is at a higher level than the export one; thus, the operating condition is stable, the grid is mainly supporting the load, and the EMS

is balancing the power flow. Moreover, the high PV self-consumption rate indicates that the renewable generation is being effectively utilized within the microgrid.

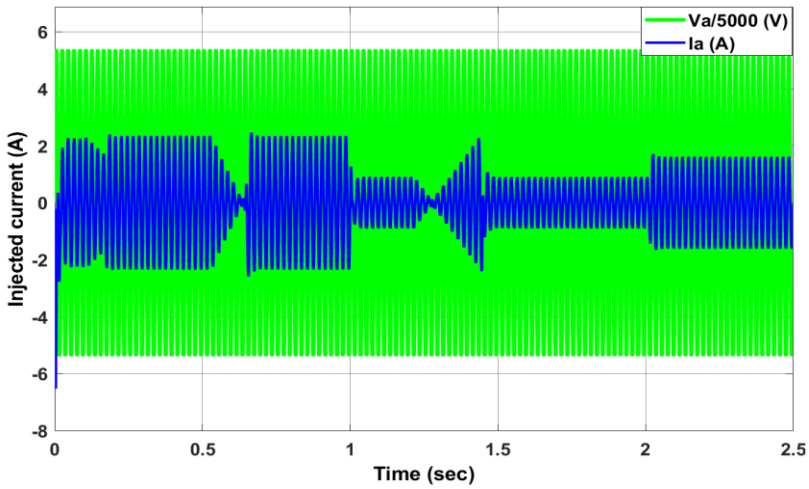

Figure 13. Grid voltage and current at scenario 1

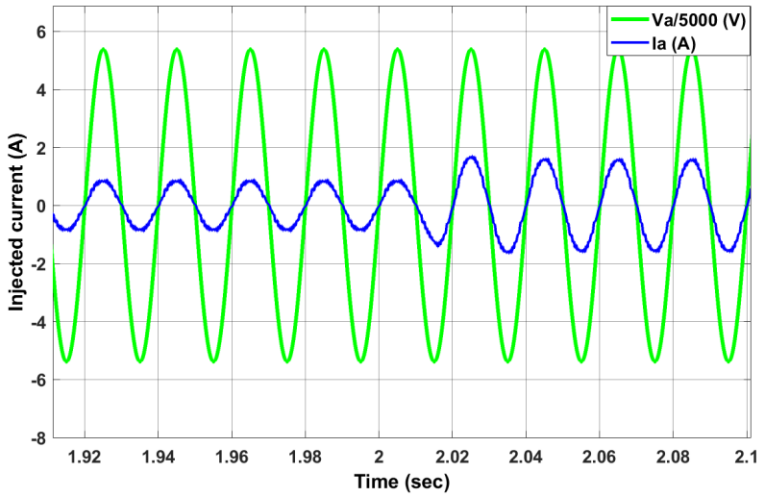

Figure 14. Zoom result of grid current

Table 2. Obtained results at case study 1

Parameter	Value
DC bus voltage	$V_{dc,ref} = 700\ V$
Max. DC bus voltage	$V_{dc,Max} = 760\ V$
Min. DC bus voltage	$V_{dc,min} = 660\ V$
Overshoot voltage	7%
Undershoot voltage	5%
PV self-consumption	80%
Power factor	0.99 %
THD	0.45 %

4.2 Case study 2: Cloudy irradiance evaluation

In this section, only the solar irradiance is changed as shown in Figure 15. This profile was added to represent the cloudy irradiance during the day. This profile was used to show the performance of the EMS under different weather conditions. Moreover, the achieved results under this scenario are reported in Figure 16. The DC bus voltage has been regulated via the EMS by ensuring a minimum overshot and high dynamic response to the changes in the irradiance. The real power of all sources are varied according to the PV generation due to the consumption EV is still same. The electrical load at time interval ($0\ sec - 0.5\ sec$) is 40 kW, ich is more than the generated power from the PV panels, therefore, the required demand is absorbed from the grid while the ESU keeps in charging operation. After this period, the PV power increases due to the increasing the irradiation. The electrical load stays without changing and the EV load is zero, therefore the required power and charging operation for the ESU are absorbed from the PV system. Between intervals ($0.5\ sec - 2\ sec$), the PV productivity is high and so the required power is covered, and the excess is exported to the grid as observed in the injected current. During this interval, the BSU can support the EV load based on its SOC limits. Lastly, the EMS successfully optimizes the generation sources, load demand, and charges the BSU by managing the power and controls the reference power conditions. The findings confirm that the LF-ANN can improve the power quality of the grid-tied system via controlled the dq-axis power as shown in Figure 16(d).

Furthermore, the active and reactive power of the grid under case 2 is shown in Figure 17. In this figure, the grid can support the load by providing a required active power and cancelled reactive power component. This means the EMS of the grid is robustness and the system can share or drawn power from the

grid based on the PV generation or load consumption. Figure 18 shows the grid current with its voltage. Figure 19 displays the zoom of the achieved results under this scenario. As observed, the grid current to at a time interval ($2.05\ sec - 2.16\ sec$) was injected to the grid. The RMS value of this current ais bout $2\ A$. At this interval, the reactive power is exported into the grid due to the consumption is low and the BSU is within the same SOC. At same time, the PV power is high and therefore all demand covered by the renewable energy source. Against, the injected current at interval ($2.16\ sec - 2.27\ sec$) was shifts by 180° relative to the corresponding grid voltage. This indicates a reversal power flow and the real power consumed from the grid. As observed, the peak RMS current is reduced based on the required absorption value. The transient in the current occurs smoothly with absence high overshoot or distortion, ensuring the accuracy of the grid-tied control scheme and the performance of the LF-ANN method. Table 3 displays the obtained results at case study 2.

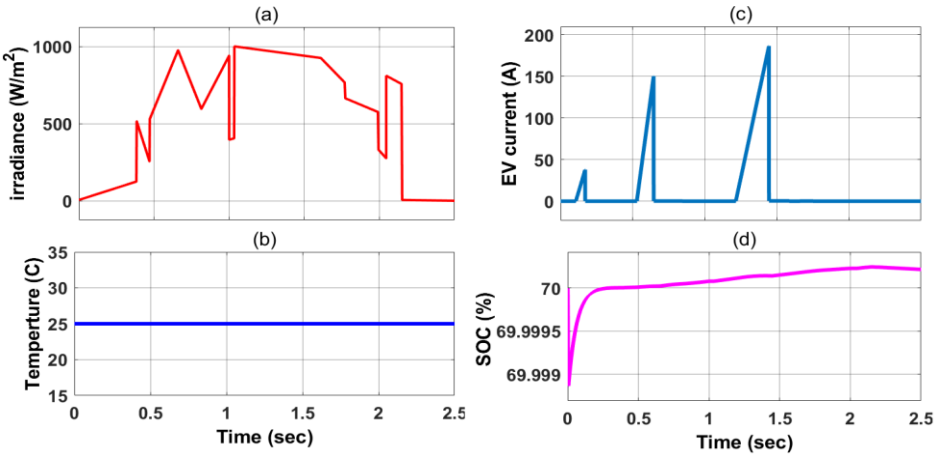

Figure 15. (a) Cloudy irradiance profile, (b) temperature, (c) electric vehicle (EV) current, (d) state-of-charge (SOC) of the BSU under scenario 2

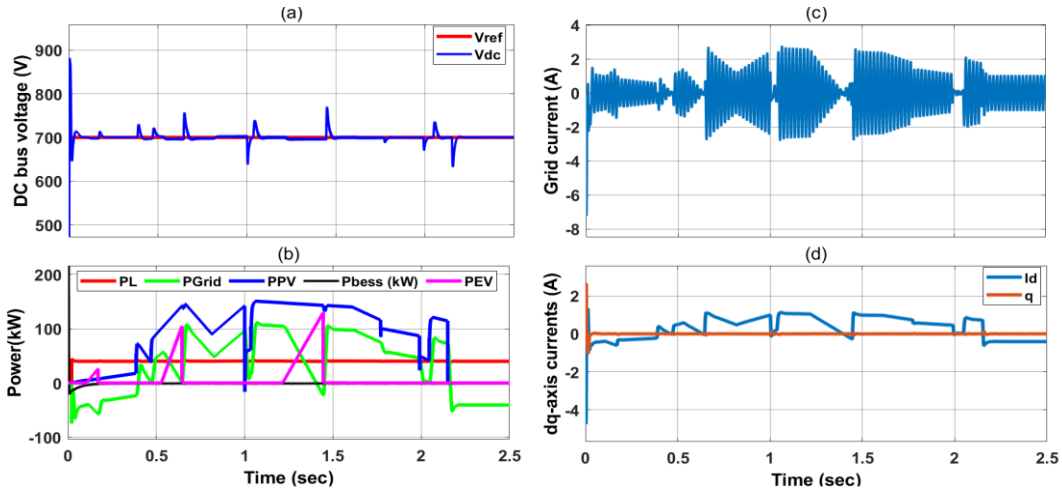

Figure 16. (a) DC bus voltage, (b) active power of system, (c) injected current to grid, (d) dq-axis currents under scenario 2

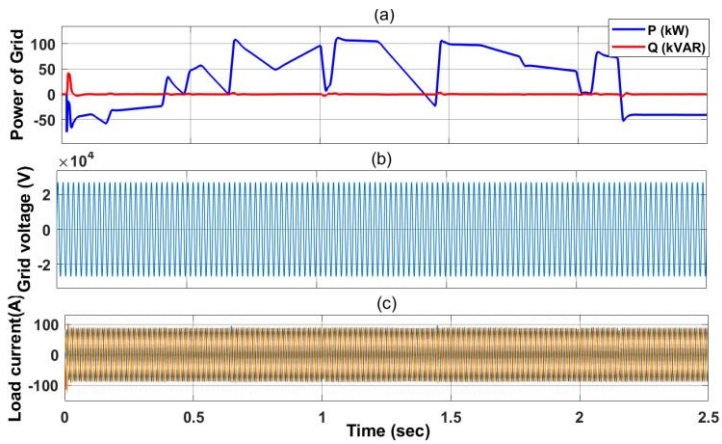

Figure 17. (a) Active reactive power of the grid, (b) high voltage side of the grid, (c) electrical load power under scenario 2

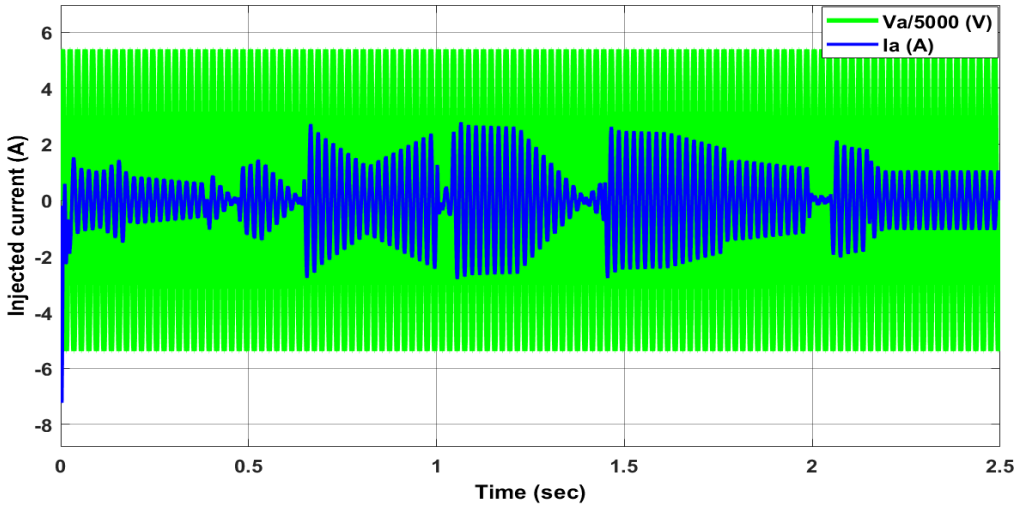

Figure 18. Injected current to the grid

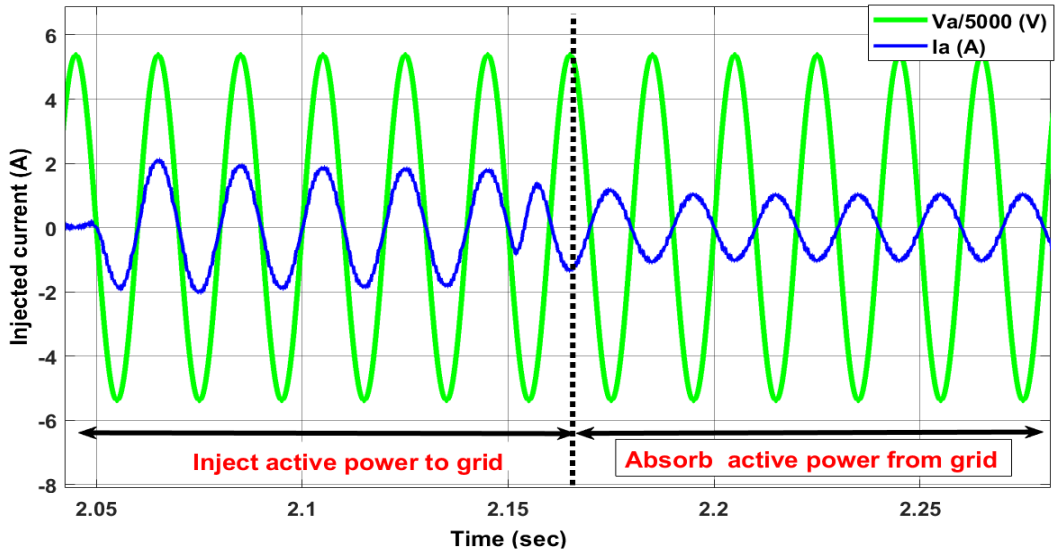

Figure 19. Zoom out of the injected current

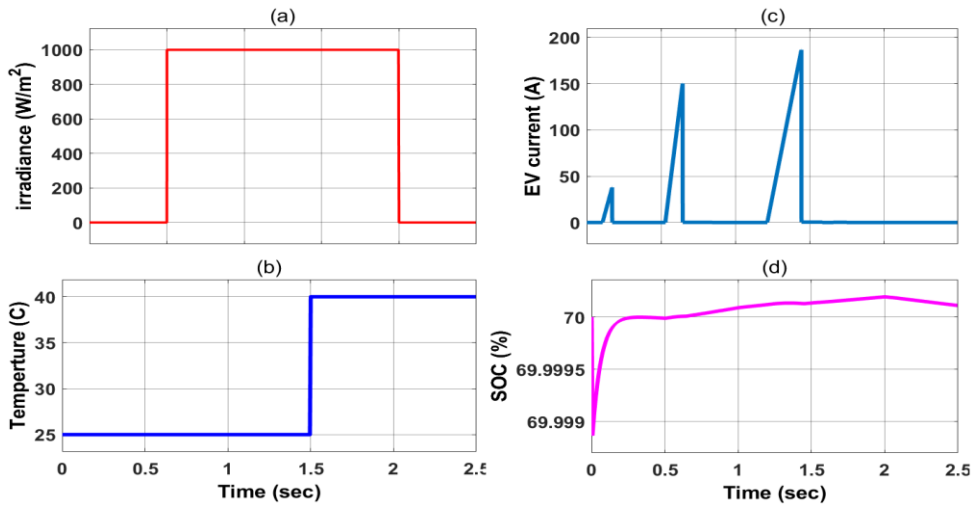

Figure 20. (a) Irradiance graph, (b) temperature, (c) electric vehicle (EV) current, (d) state-of-charge (SOC) of the battery under scenario 3

Table 3 presents a summary of the performances of the proposed LF ANN EMS under case study 2. The DC-link voltage is tightly regulated around the nominal value of 700 V, with the controller limiting the voltage excursions to the upper bound (790 V) and lower bound (640 V), which is a strong indication that the closed-loop system remains stable

under the influence of operation disturbances. The overshoot (7.8%) and undershoot (5.5%) reported here illustrate a well-damped dynamic behavior, and the transient deviation is thus sufficiently small for the DC microgrid operation. The grid power factor is kept at a high level (PF ≈ 0.98), which means that there has been an almost total disappearance of reactive power, and thus the power exchanged between the converter and the grid is actually active power only. Furthermore, the current distortion is extremely low (THD ≈ 0.6%), which indicates that the injected current is practically a pure sinusoid and that there is strong adherence to the grid power quality standards. The whole set of results points to the fact that the proposed EMS is very effective in maintaining voltage stability as well as in enhancing the grid-side power quality.

Table 3. Obtained results at case study 2

Parameter	Value
DC bus voltage	$V_{dc,ref} = 700\ V$
Max. DC bus voltage	$V_{dc,Max} = 790\ V$
Min. DC bus voltage	$V_{dc,min} = 640\ V$
Overshoot voltage	7.8%
Undershoot voltage	5.5%
PV self-consumption	520%
Power factor	0.98 %
THD	0.6 %

4.3 Case study 3: Variable weather and step increasing in AC load

In this section, both irradiance and cell temperature are varied with step changes conditions as shown in Figure 20. Moreover, the goal of this case is to validate the suggested EMS under different operation conditions related to the PV generation and load consumption.

Figure 21 introduces the obtained results under varying weather and load conditions. AS observed, the DC voltage regulation via the EMS is achieved. The ripple content or fluctuating in the measured voltage stay within limits. The deviation in the voltage less than 4%, and this confirms the EMS working by controls the derivative of the bus voltage $\dot{V}_{dc,bus}$ using ANN controller. the PV power from time 0.5 sec to 2 sec is very high and the BSU charging, EV load, and electrical load are covered. Before this interval the grid is covered the loads. At time $t = 1\ sec$, the electrical load is increased from 40 kW to 80 kW .at this moment, the EMS ensures the generation and compute the load consumption to provide the decision. As a result, the PV power is high and this load was converted. After some seconds at time $t = 1.2\ sec$, the load profile of the EV becomes very high as well as the electrical load is high, so the PV and grid are worked together to covers the load and charge the ESU.

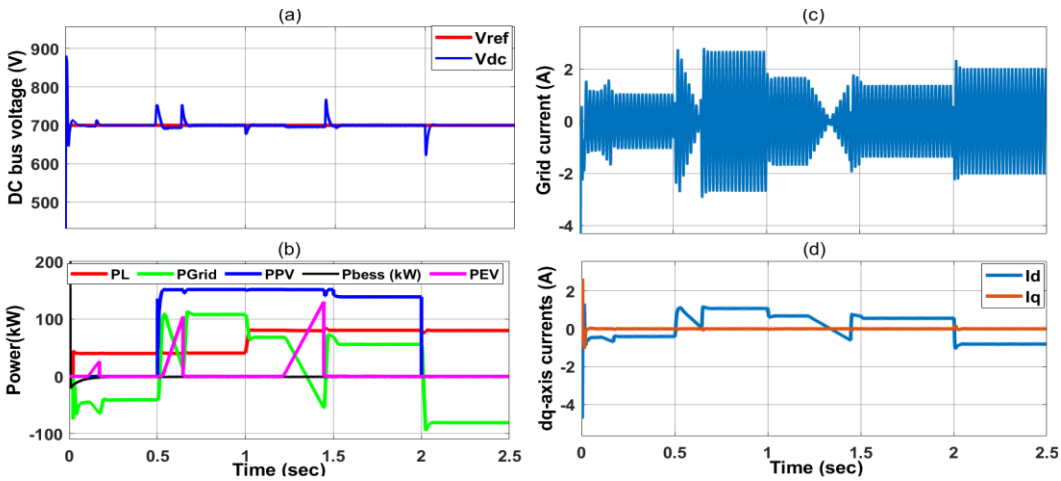

Figure 21. Obtained results under varying weather and load conditions

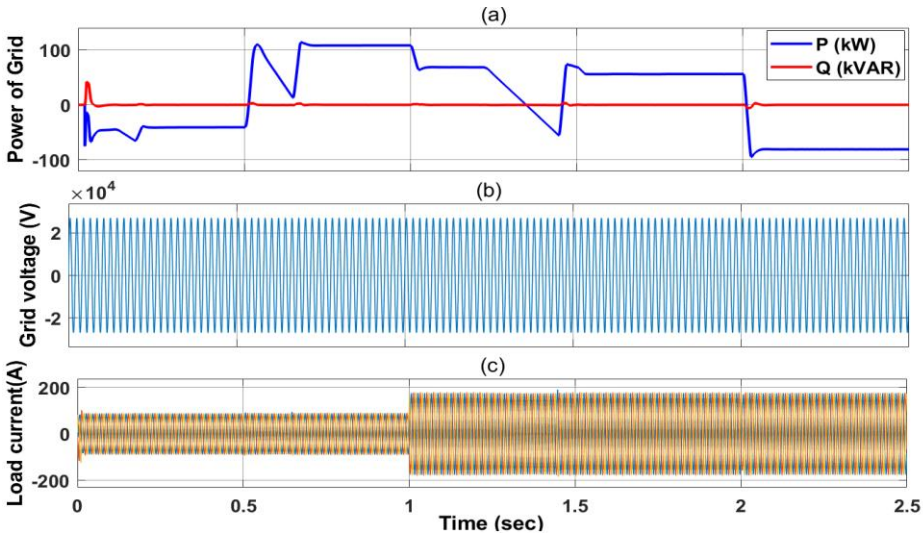

Figure 22. (a) Grid power, (b) volatge of gird, (c) electrcal load current

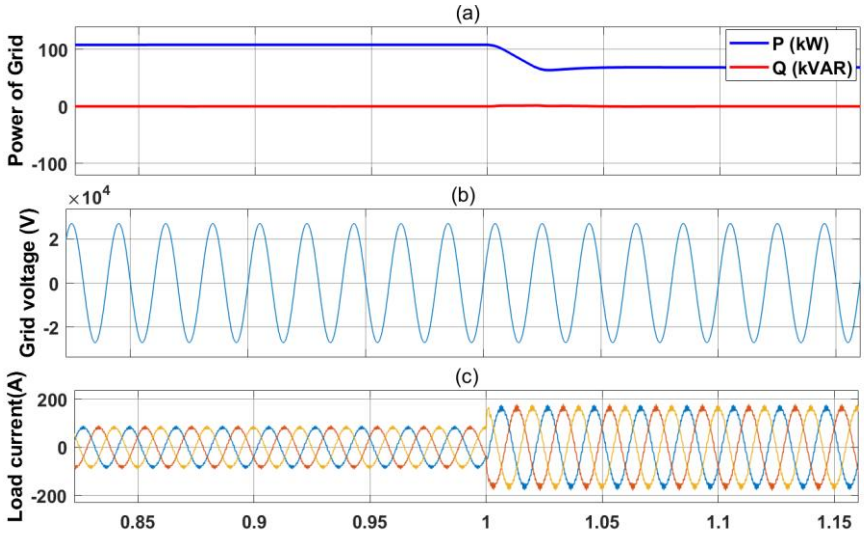

Figure 23. Zoom of the results

Figures 22 and 23 display the grid power, volatge and current of the elctrical load. Also, the zoom of this result was shown in Figure 23. As observed, at time $t = 1\ sec$, the electrical load current is increased from 80 A to 175 A. The grid voltage keeps constant with 33 KV. The increasing in the load may cause the power flow changes from the positive to negative. At him moment, the grid power keeps positive (export power) due to the PV power is high. Moreover, this can be seen in the injected current as shown in Figures 24 and 25.

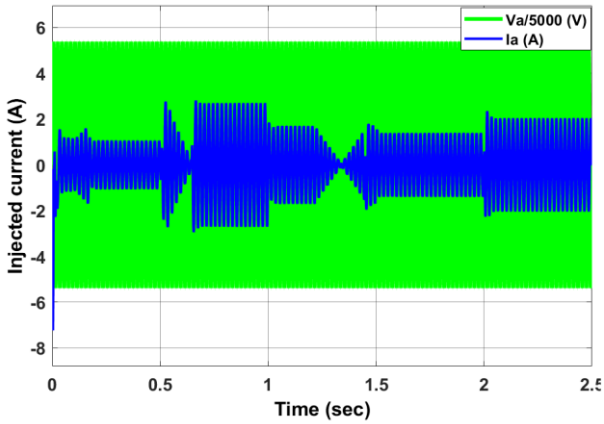

Figure 24. The injected current to the grid

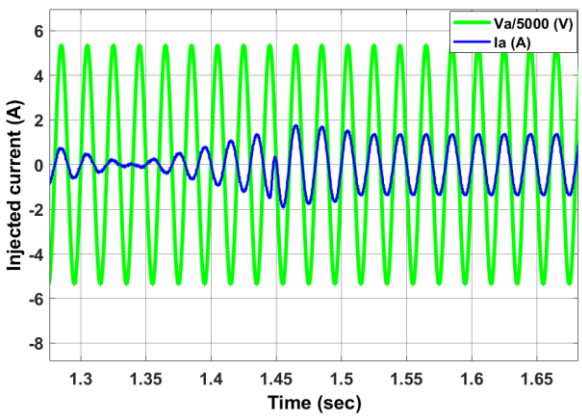

Figure 25. Zoom of the injected current

Table 4 reports the obtained results at case study 3. Although the voltage of the DC bus is showing a bit more overshoot/undershoot, this variation is due to the very rapid changes in load and renewable generation. However, it is still within perfectly acceptable limits and is very fast in coming back to the reference value. The grid power factor stays very close to unity (PF > 0.99), which is evidence that the reactive power exchange has been kept at an absolute minimum even during a very dynamic operation. The grid actively participates in maintaining system stability, as evidenced by the grid import/export energy figures. Meanwhile, the PV self-consumption ratio of approximately 69% indicates that a significant portion of locally generated renewable energy is consumed locally, demonstrating the potential of EMS for coordinated energy dispatch.

Table 4. Obtained results at case study 3

Parameter	Value
DC bus voltage	$V_{dc,ref} = 700\ V$
Max. DC bus voltage	$V_{dc,Max} = 770\ V$
Min. DC bus voltage	$V_{dc,min} = 635\ V$
Overshoot voltage	10%
Undershoot voltage	7.7%
PV self-consumption	69%
Power factor	0.99%
THD	0.57%

4.4 Comparison with the classical load-following method

To prove the effectiveness of the proposed EMS, the comparison between the results achieved in the classical LF-PI method and the suggested EMS is done. Therefore, the DC bus voltage curves under the third case was selected to compare the performance. In this case, the irradiance, temperature, and electrical load are varied as shown in previous section (case 3). Figure 26 shows the response of the proposed EMS and the classical LF-PI method. The comparison in terms of the DC bus response for the three cases is presented. Then, the overshoot, settling time, and rise time are shown to verify the comparison and displays the best performance as displays in Table 5. As observed, the proposed EMS offers less overshoot and fast time convergence especially when the irradiance changed in time 0.5 sec, while

the classical method severs from the unwanted high spikes in the DC voltage, which presents energy loss in the system and lowered the overall efficiency.

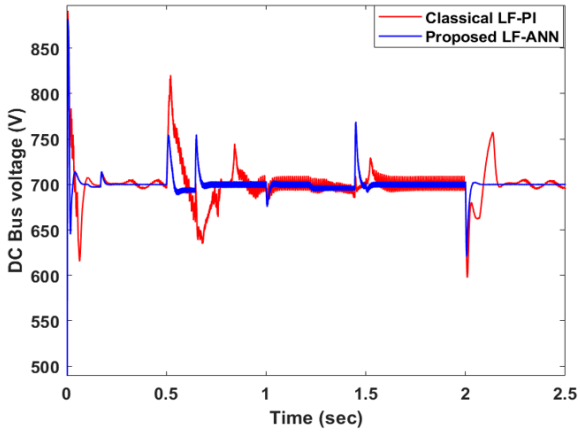

Figure 26. DC bus voltage curve under both classical and proposed energy management strategy (EMS)

Table 6 reports a comparative analysis of the proposed EMS with state of arts methods. The comparison was conducted in terms of the complexity, degree of the voltage stability, and type of the configuration structure. From this table, the suggested LF-ANN EMS allows for very simple low-complexity for real-time energy dispatch. It requires less inputs, thus achieving fast DC-link stabilization, near-unity PF with very low THD, and stringent performance under PV/EV/grid operating scenarios without the need for forecasting or communication infrastructure.

Table 5. Comparison between the proposed energy management strategy (EMS) and the classical method

Case Study	EMS Method	Settling Time (sec)	Rise Time (sec)	Overshoot (V)	Undershoot (V)
Case 1	Proposed EMS	0.11	0.034	56	66
	Classical EMS	0.16	0.043	60	98
Case 2	Proposed EMS	0.09	0.032	44	55
	Classical EMS	0.12	0.03	120	95
Case 3	Proposed EMS	0.1	0.04	50	60
	Classical EMS	0.15	0.08	150	100

Table 6. Comparison with recent state-of-arts energy management strategy (EMS) methods

Method	System Configuration	Voltage Stability	Limitations	Complexity
EMS based optimization [10]	PV/WT/BESS/Grid/EV	Good	Proposes optimal sizing and control of grid-connected microgrid.	High
ANFIS [11]	BESS/Grid/ EV (V2G)	Good	ANFIS design depends on rule base & membership tuning; scalability and reproducibility may be limited.	Moderate
ANN [12]	PV/grid/BESS	Medium	ANN performance is substantially determined by the training data.	Moderate
AI based EMS [13]	Grid/EV(V2G)	Good	V2H scheduling mostly, limited microgrid level dynamics and converter level validation.	High
Rule-based EMS [16]	PV/Grid/EV(V2G)	Low	Optimize the cost or battery aging are not considered.	Low
AI-EMS [17]	PV/grid/EV	Good	Sever from a high computational time	High
Dynamic AI-EMS [18]	PV/BESS/grid/EV load	Good	Due to the limited intelligence, it is less capable than AI-based EMS.	Moderate
Flatness EMS [19]	PV/BESS	Good	Requires accurate modeling/flatness formulation.	High
Hybrid control [22]	BESS/SC	Good		
PI-EMS [25]	Hydrogen Fuel cell/BESS/PV	Good	Needs FC dynamics and a hydrogen system and more expensive.	High
LF-EMS [27]	Fuel cell/ PV	Low	The authors not consider power quality indices (THD and PF).	Low
Proposed LF-ANN	PV/BESS/Grid/EV load	Very good	The EMS provides a fast DC-link stabilization and good power quality under different weather conditions.	Low

5. CONCLUSION AND FUTURE WORK

In this article, a LF-ANN-based EMS is proposed to supply EV demand with a renewable microgrid. The hybrid DC/AC microgrid under the study includes in its configuration a solar PV source, a battery energy storage system (BESS), AC loads, an EV load profile. The proposed EMS was tested and validated in MATLAB/Simulink under various case studies, including variable weather and load demand levels. According to the simulation results, the LF-ANN strategy stabilizes the DC-bus voltage and ensures the power sharing between PV, BESS, and the utility grid. Besides that, the proposed EMS is capable of maximizing the use of the PV energy and also enhancing the overall system performance while BESS continues to operate efficiently. The achieved results are analyzed in terms of the DC bus voltage regulation, exportation or absorption the active power from the grid and optimizing the demand load consumption. The EMS confirms high dynamic response, less oscillation in the DC bus voltage and well tracking efficiency of the PV system. The achieved results are compared with those collected from the classical EMS under different scenarios. Finally, the suggested EMS presents less overshoot, fast settling time, faster in rise time when compared with classical EMS under complex operation conditions.

The ECE-Urban drive cycle was utilized to produce a time-varying EV power profile, thus representing the real fluctuations in EV charging/consumption demand and its

effects on DC-bus stability and grid interaction. Future work will involve extending the proposed LF-ANN EMS to a fully bidirectional V2G/G2V operation through modeling of EV arrival/departure events, minimum departure SOC constraints, and bidirectional converter limits.

REFERENCES

[1] Chen, L., Ma, R. (2024). Clean energy synergy with electric vehicles: Insights into carbon footprint. Energy Strategy Reviews, 53: 101394. https://doi.org/10.1016/j.esr.2024.101394

[2] De Schepper, E., Van Passel, S., Lizin, S. (2015). Economic benefits of combining clean energy technologies: The case of solar photovoltaics and battery electric vehicles. International Journal of Energy Research, 39(8): 1109-1119. https://doi.org/10.1002/er.3315

[3] Requia, W.J., Mohamed, M., Higgins, C.D., Arain, A., Ferguson, M. (2018). How clean are electric vehicles? Evidence-based review of the effects of electric mobility on air pollutants, greenhouse gas emissions and human health. Atmospheric Environment, 185: 64-77. https://doi.org/10.1016/j.atmosenv.2018.04.040

[4] Munsi, M.S., Chaoui, H. (2024). Energy management systems for electric vehicles: A comprehensive review of technologies and trends. IEEE Access, 12: 60385-60403. https://doi.org/10.1109/ACCESS.2024.3371483

[5] Challoob, A.F., Bin Rahmat, N.A., A/L Ramachandaramurthy, V.K., Humaidi, A.J. (2025). Robust energy management system for electric vehicle. International Review of Applied Sciences and Engineering, 16(1): 98-117. https://doi.org/10.1556/1848.2024.00839

[6] Guille, C., Gross, G. (2009). A conceptual framework for the vehicle-to-grid (V2G) implementation. Energy Policy, 37(11): 4379-4390. https://doi.org/10.1016/j.enpol.2009.05.053

[7] Shariff, S.M., Iqbal, D., Alam, M.S., Ahmad, F. (2019). A state of the art review of electric vehicle to grid (V2G) technology. IOP Conference Series: Materials Science and Engineering, 561(1): 012103. https://doi.org/10.1088/1757-899X/561/1/012103

[8] Mojumder, M.R.H., Ahmed Antara, F., Hasanuzzaman, M., Alamri, B., Alsharef, M. (2022). Electric vehicle-to-grid (V2G) technologies: Impact on the power grid and battery. Sustainability, 14(21): 13856. https://doi.org/10.3390/su142113856

[9] Sovacool, B.K., Axsen, J., Kempton, W. (2017). The future promise of vehicle-to-grid (V2G) integration: A sociotechnical review and research agenda. Annual Review of Environment and Resources, 42(1): 377-406. https://doi.org/10.1146/annurev-environ-030117-020220

[10] Ouramdane, O., Elbouchikhi, E., Amirat, Y., Sedgh Gooya, E. (2021). Optimal sizing and energy management of microgrids with vehicle-to-grid technology: A critical review and future trends. Energies, 14(14): 4166. https://doi.org/10.3390/en14144166

[11] Shakeel, F.M., Malik, O.P. (2022). ANFIS based energy management system for V2G integrated micro-grids. Electric Power Components and Systems, 50(11-12): 584-599. https://doi.org/10.1080/15325008.2022.2138638

[12] Sathyan, S., Pandi, V.R., Antony, A., Salkuti, S.R., Sreekumar, P. (2024). ANN-based energy management system for PV-powered EV charging station with battery backup and vehicle to grid support. International Journal of Green Energy, 21(6): 1279-1294. https://doi.org/10.1080/15435075.2023.2246048

[13] Shamami, M.S., Alam, M.S., Ahmad, F., Shariff, S.M., AlSaidan, I., Rafat, Y., Asghar, M.J. (2020). Artificial intelligence-based performance optimization of electric vehicle-to-home (V2H) energy management system. SAE International Journal of Sustainable Transportation, Energy, Environment, & Policy, 1(13-01-02-0007): 115-125. https://doi.org/10.4271/13-01-02-0007

[14] Singh, A.P., Kumar, Y., Sawle, Y., Alotaibi, M.A., Malik, H., Marquez, F.P.G. (2024). Development of artificial intelligence-based adaptive vehicle to grid and grid to vehicle controller for electric vehicle charging station. Ain Shams Engineering Journal, 15(10): 102937. https://doi.org/10.1016/j.asej.2024.102937

[15] Gogoi, D., Bharatee, A., Ray, P.K. (2024). Implementation of battery storage system in a solar PV-based EV charging station. Electric Power Systems Research, 229: 110113. https://doi.org/10.1016/j.epsr.2024.110113

[16] Haque, A., Kurukuru, V.S.B., Khan, M.A. (2019). Energy management strategy for grid connected solar powered electric vehicle charging station. In 2019 IEEE Transportation Electrification Conference (ITEC-India), Bengaluru, India, pp. 1-6. https://doi.org/10.1109/ITEC-India48457.2019.ITECINDIA2019-44

[17] Amir, M., Zaheeruddin, Haque, A., Bakhsh, F.I., Kurukuru, V.B., Sedighizadeh, M. (2024). Intelligent energy management scheme-based coordinated control for reducing peak load in grid-connected photovoltaic-powered electric vehicle charging stations. IET Generation, Transmission & Distribution, 18(6): 1205-1222. https://doi.org/10.1049/gtd2.12772

[18] Kouka, K., Masmoudi, A., Abdelkafi, A., Krichen, L. (2020). Dynamic energy management of an electric vehicle charging station using photovoltaic power. Sustainable Energy, Grids and Networks, 24: 100402. https://doi.org/10.1016/j.segan.2020.100402

[19] Yaqoob, S.J., Ferahtia, S., Obed, A.A., Rezk, H., Alwan, N.T., Zawbaa, H.M., Kamel, S. (2022). Efficient flatness based energy management strategy for hybrid supercapacitor/lithium-ion battery power system. IEEE Access, 10: 132153-132163. https://doi.org/10.1109/ACCESS.2022.3230333

[20] Vu, L., Nguyen, T.T., Nguyen, B.L.H., Anam, M.I., Vu, T. (2024). Real-time hybrid controls of energy storage and load shedding for integrated power and energy systems of ships. Electric Power Systems Research, 229: 110191. https://doi.org/10.1016/j.epsr.2024.110191

[21] Rezk, H., Ghoniem, R.M. (2023). Optimal load sharing between lithium-ion battery and supercapacitor for electric vehicle applications. World Electric Vehicle Journal, 14(8): 201. https://doi.org/10.3390/wevj14080201

[22] Challoob, A.F., Rahmat, N.A.B., Ramachandaramurthy, V.K., Saeed, N., Humaidi, A.J. (2024). An intelligent battery management system for an electric vehicle powered by solar PV array. In 2024 59th International Universities Power Engineering Conference (UPEC),

Cardiff, United Kingdom, pp. 1-6. https://doi.org/10.1109/UPEC61344.2024.10892594
[23] Yaqoob, S.J., Hussein, A.R., Saleh, A.L. (2020). Low cost and simple P&O-MPP tracker using flyback converter. Solid State Technology, 63(6): 9676-9689.
[24] Nagaraju, S., Ramaswamy, N.K., Ramaswamy, R.K. (2023). Design and implementation of hybrid controller for dynamic power management in a DC Microgrid. Journal of Intelligent Systems and Control, 2(1): 1-12. https://doi.org/10.56578/jisc020101
[25] Thounthong, P., Sikkabut, S., Mungporn, P., Piegari, L., Nahid-Mobarakeh, B., Pierfederici, S., Davat, B. (2015). DC bus stabilization of li-ion battery based energy storage for a hydrogen/solar power plant for autonomous network applications. IEEE Transactions on Industry Applications, 51(4): 2717-2725. https://doi.org/10.1109/TIA.2015.2388853
[26] Yaqoob, S.J., Arnoos, H., Qasim, M.A., Agyekum, E.B., Alzahrani, A., Kamel, S. (2023). An optimal energy management strategy for a photovoltaic/Li-ion battery power system for DC microgrid application. Frontiers in Energy Research, 10: 1066231. https://doi.org/10.3389/fenrg.2022.1066231
[27] Bizon, N. (2014). Load-following mode control of a standalone renewable/fuel cell hybrid power source. Energy Conversion and Management, 77: 763-772. https://doi.org/10.1016/j.enconman.2013.10.035
[28] Bizon, N., Oproescu, M., Raceanu, M. (2015). Efficient energy control strategies for a standalone renewable/fuel cell hybrid power source. Energy Conversion and Management, 90: 93-110. https://doi.org/10.1016/j.enconman.2014.11.002
[29] Ghosh, S.K., Roy, T.K., Pramanik, M.A.H., Sarkar, A.K., Mahmud, M.A. (2020). An energy management system-based control strategy for DC microgrids with dual energy storage systems. Energies, 13(11): 2992. https://doi.org/10.3390/en13112992